

Geophysical Research Letters

RESEARCH LETTER

10.1029/2019GL086419

Key Points:

- Numerical simulations show that on average, approximately 10% of the cusp O⁺ outflow may land in the plasma sheet and change tail dynamics
- Numerical experiments show that cusp O⁺ outflow alone can induce magnetospheric sawtooth oscillations with CME-type driving conditions
- Theoretically, neither nightside outflow nor outflow feedback loops are required to generate magnetospheric sawtooth oscillations

Correspondence to:

B. Zhang,
binzh@hku.hk

Citation:

Zhang, B., Brambles, O. J., Lotko, W., & Lyon, J. G. (2020). Is nightside outflow required to induce magnetospheric sawtooth oscillations. *Geophysical Research Letters*, 47, e2019GL086419. <https://doi.org/10.1029/2019GL086419>

Received 26 NOV 2019

Accepted 31 DEC 2019

Accepted article online 3 JAN 2020

Is Nightside Outflow Required to Induce Magnetospheric Sawtooth Oscillations

Binzheng Zhang^{1,2} , Oliver J. Brambles³, William Lotko^{2,4} , and John G. Lyon⁵

¹Department of Earth Sciences, the University of Hong Kong, Pokfulam, Hong Kong SAR, China, ²High Altitude Observatory, National Center for Atmospheric Research, Boulder, CO, USA, ³Preston, UK, ⁴Thayer School of Engineering, Dartmouth College, Hanover, NH, USA, ⁵Department of Physics and Astronomy, Dartmouth College, Hanover, NH, USA

Abstract Ionospheric outflow plays an important role in the mass coupling between the ionosphere and the coupled solar wind-magnetosphere system. Previous modeling studies have shown that outflowing ionospheric ions may induce magnetospheric sawtooth oscillations through mass loading of the magnetotail, stretching the magnetic field lines, and reducing nightside reconnection. The spatial distribution of polar cap outflow in these simulation studies produces significant outflow in the auroral oval and lacks a distinct cusp source. Thus, the question arises whether cusp outflow can induce sawtooth oscillations. We show controlled numerical experiments with magnetospheric sawtooth oscillations induced by an idealized cusp outflow for driving conditions representative of the interaction of an interplanetary coronal mass ejection with Earth's magnetosphere. The analysis shows that although only a small portion (10%) of the cusp outflow is entrained within the plasma sheet, it is effective in inducing magnetospheric sawtooth oscillations, similar to previous experiments.

1. Introduction

Magnetospheric sawtooth oscillations were first observed more than two decades ago (e.g., Borovsky et al., 1993). The oscillations exhibit electron fluxes versus time at geostationary orbit that resemble the teeth of a saw blade, with a periodic sequence of slow decrease in flux followed by a rapid increase (e.g., Belian et al., 1995). This signature is observed over a broad range of magnetic local time (MLT), up to 12 hr or more, and is used to distinguish the associated sawtooth substorms from isolated substorms. Other geospace diagnostics have since been shown to vary synchronously with these periodic injections: Magnetic field variations at geostationary orbit, in the tail and at ground stations; auroral electrojet index; auroral precipitation index; and polar cap index (e.g., Cai et al., 2006; Henderson et al., 2006; Huang et al., 2003; Kitamura et al., 2005; Troshichev & Janzhura, 2009). Although the mechanism or mechanisms exciting the magnetospheric sawtooth mode are still an open question, numerical simulations of the coupled magnetosphere-ionosphere system have demonstrated a possible causal pathway involving ionospheric O⁺ outflows. Sufficiently profuse outflows induce a relaxation oscillation in the substorm cycle that periodically mass loads the plasma sheet and alters the magnetotail reconnection rate (e.g., Brambles et al., 2011; Varney et al., 2016a, 2016b).

Wiltberger et al. (2010) used a multifluid magnetohydrodynamic simulation to demonstrate that when outflowing cusp ions land near the site of nightside reconnection and become entrained within the plasma sheet, the nightside field lines are stretched beyond a critical point for maintaining topological similarity in the magnetic geometry. Beyond this point, a substorm dipolarization occurs with an accompanying plasmoid being released downtail. Similar dynamics were observed in other simulations when the cusp outflow was specified to be sufficiently slow (Brambles et al., 2010). In both studies, after release of the plasmoid, the magnetotail was reconfigured with the nightside reconnection X-line moving earthward. The continuing cusp outflow subsequently landed downstream of the new nightside reconnection line, did not interact further with the site of reconnection, and did not induce any subsequent substorms. Global multifluid simulations from another global magnetosphere model have also shown similar influence of cusp O⁺ outflows on the development of isolated substorms (Yu & Ridley, 2013).

Brambles et al. (2011) showed that the introduction of a causally driven, semiempirically specified ionospheric outflow in a multifluid magnetohydrodynamic simulation can induce quasiperiodic substorms

resembling observed sawtooth oscillations with a recurrence period of 2–4 hr. The maximum magnetic inclination angle at geostationary orbit was found to be larger than in an isolated substorm, with a broader MLT distribution. The outflow at the inner simulation boundary ($2 R_E$ geocentric) was regulated using an empirical power law relationship derived from FAST measurements, which gives the ionospheric outflow flux as a function of Alfvénic Poynting flux. The resulting outflow peaked around the nightside auroral oval and extended in MLT to the dawn-dusk meridian. The Brambles et al. (2011) simulations lacked a distinct cusp outflow population due to the idealized, steady southward interplanetary magnetic field conditions driving the magnetosphere. Steady driving stimulates negligible Alfvénic power flowing into the high-altitude cusp (Zhang et al., 2014), so the empirical power law relation between outflow flux and Poynting flux produced negligible cusp outflow in the simulation. This study also suggested that sawtooth oscillations do not occur if the hemispheric outflow rate (outflow flux integrated over the simulation hemisphere) is too low. As the hemispheric outflow rate decreased (due to either weaker interplanetary driving or artificially downscaling the empirical outflow relationship), the sawtooth period increased and the sawtooth amplitude progressively decreased to the point where the resulting dynamic state was indistinguishable from a steady magnetospheric convection state.

In a follow-up study, Ouellette et al. (2013) analyzed the sawtooth substorms simulated by Brambles et al. (2011), in particular the change the ion composition of the plasma sheet and magnetotail due to the cusp O^+ outflow and its effect on the nightside reconnection rate. The increase in mass density and accompanying decrease in Alfvén speed in the lobe reconnection inflow reduces the tail reconnection rate in the simulation, leading to an accumulation of open flux in the magnetotail and an imbalance between dayside and nightside reconnection rates. When the open flux reaches a critical level, it rapidly reconnects and produces a substorm. This process repeats leading to periodic substorms. Even though the largest outflow fluxes emerged from the nightside auroral zone in these simulations, Ouellette et al. (2013) reported that the bulk of the outflow populating the midtail plasma sheet and interacting directly with nightside reconnection entered the simulation domain near dawn and dusk MLT (their Figure 6). They also observed a burst of outflow caused by increased Alfvénic power stimulated by the breakup of the magnetotail during the expansion phase of the simulated sawtooth substorms. It was hypothesized that this massive outflow inflates the magnetotail and allows the development of the next sawtooth oscillation. This inflation-deflation cycle differs from the outflow-induced substorm described by Wiltberger et al. (2010), wherein the magnetotail was internally reconfigured to a state that suppresses further outflow-induced substorms.

Periodic magnetospheric oscillations also occur in global magnetosphere simulations coupled with a physics-based ionospheric outflow model (Varney et al., 2016a, 2016b). The model includes an ion conic distribution representing a nonthermal outflow energized by Alfvénic power flowing into the ionosphere, with energization regulated by Poynting flux dynamically derived from the global magnetosphere model (Zhang et al., 2012). For idealized CME-like driving conditions, Varney et al.'s O^+ energization model produces outflow throughout the auroral oval and polar cap with a peak flux on the nightside. Sawtooth-like oscillations were more likely to be excited in these simulations with increased nightside outflow; however, the resulting sawtooth substorms had a smaller change in open flux (≈ 0.1 GWb per cycle) compared to the open flux in observations and in the Brambles et al. (2011) study (≈ 0.2 GWb). The mean sawtooth period of 75 min was also shorter. Varney et al. (2016b) suggested that causally driven nightside outflow involving a burst of outflow during the expansion phase was required to produce sawtooth oscillations. This conjecture is partially based on the fact that previous simulations with either fixed cusp outflow (Wiltberger et al., 2010) or fixed nightside outflow (Garcia et al., 2010) did not produce periodic substorms. Garcia et al. (2010) observed inflation of the magnetotail, together with formation of plasmoids in the magnetotail using a large rate of nightside O^+ outflow. However, their simulations were only run for 4 hr after preconditioning, which may not allow sufficient time for sawtooth substorms to manifest.

Using the Brambles et al. (2011) empirical outflow model, Brambles et al. (2013) investigated the impact of outflow on the mode of convection for two sawtooth events—the SIR-driven 24 October 2002 event and the CME-driven 18 April 2002 event. In both event simulations the ion outflow flux near the dayside cusp was much larger than in the idealized simulations of Brambles et al. (2011) and Varney et al. (2016b) due to the nonsteady interplanetary driving. In both events outflow was required to generate the large-amplitude and wide-in-MLT signatures in observations. However, periodic substorms occurred in the SIR event even without outflow whereas they did not occur in the simulated CME event without outflow. Evidently, the quasiperiodic substorms in the SIR event were triggered by variability in interplanetary conditions rather

than some internal process as in the CME event. Due to the complicated variations in both the upstream driving and ionospheric outflow, Brambles et al. (2013) did not isolate the role of dayside versus nightside outflow in generating magnetotail sawtooth oscillations for the CME-driven event. Note that the inclusion of nonideal MHD, kinetic physics in global simulations has generated periodic (~ 1 hr) reconnections in the magnetotail driven by CME-type upstream conditions (Kuznetsova et al., 2007) without the need for O^+ outflow; however, they are yet to produce the ~ 3 hr, global-scale quasiperiodic substorms that define the sawtooth mode or demonstrate the transition from steady to periodic magnetospheric convection states.

Lund et al. (2018) used mass composition data from the Cluster satellites to test the sawtooth outflow-substorm hypothesis that was emerging from these simulation studies. Consistent with earlier findings of Kistler (2016), they found that the dominant source of O^+ in the midtail plasma sheet during interplanetary CME events is primarily from the cusp/dayside with little coming from the nightside auroral region. The results suggested that a direct nightside auroral feedback loop may not be necessary for the generation of sawtooth oscillations, which seems in agreement with the measured O^+/H^+ ratio in the plasma sheet during storm main phase (Liao et al., 2014). This observational study contradicts the theoretical predictions of Varney et al. (2016b). They are, however, consistent with the previous simulation studies of Brambles et al. (2011) for which Ouellette et al. (2013) showed that the dominant source of O^+ at midtail locations near the nightside reconnection region (at approximately $20 R_E$) is a dawn-dusk outflow flux located mostly between 6–9 and 15–18 MLT on the dayside and that the O^+ populating the plasma sheet arrives there during the substorm growth phase rather than the expansion phase. The feedback mechanism suggested by Ouellette et al. entails an inflation of the magnetotail by nightside auroral outflow, which allows further dayside-sourced ions to interact with nightside reconnection. The nightside outflow in this scenario preconditions the plasma sheet and effectively enables sawtooth behavior rather than directly causing it.

The current paper addresses two questions raised by the previous studies: Can cusp outflows excite the sawtooth mode? Is a source of nightside outflow required to enable sawtooth oscillations? The previous simulations either lacked a distinct feature of cusp outflow (as a consequence of idealized driving conditions) or mix the effects of dayside and nightside outflow. Since cusp O^+ outflows appear to be the dominant source of O^+ in the midtail plasma sheet during CME-driven storms, the present study focuses specifically on their effects. We show that magnetospheric sawtooth oscillations can be induced solely by cusp O^+ outflows in global simulations. The results also answer the second question in the negative: Nightside outflows are not required to enable sawtooth oscillations.

We present results from a multifluid MHD simulation including a causally located cusp outflow with constant outflow flux. Model information including the cusp outflow simulation setup is first described (section 2). Simulation diagnostics, analysis, and interpretations, with comparisons to previous numerical modeling and observations, are presented (section 3) to support our principal conclusions (section 4).

2. Simulation Information

We use the multifluid extension of the Lyon-Fedder-Mobarry global magnetosphere model to study the impact of ionospheric outflow on the solar wind-magnetosphere-ionosphere interaction. The numerical schemes used in solving the MHD equations are described by Lyon et al. (2004) and Zhang et al. (2019). The multifluid version of the code solves for multiple ion fluids allowing separate ionospheric-sourced ion populations to be tracked (Brambles et al., 2010). The finite volume techniques allow the numerical model to complete the calculations on a nonorthogonal curvilinear grid that is adapted to magnetospheric problems. In order to compare with the Brambles et al. (2011) results, we used the same nonuniform grid resolution, which is approximately $0.25 R_E$ near the dayside magnetopause and $0.35 R_E$ in the inner magnetosphere. Magnetic reconnection in the code occurs via numerical resistivity (Lyon et al., 2004), which is enabled only when the scales of magnetic field gradients approach the local grid size, for example, two opposite flux tubes entering the same computation cell. The reconnection electric field is typically of the order of $0.1 v_A B_{in}$, where v_A and B_{in} are the Alfvén speed and magnetic field strength in the inflow region, respectively, indicating that Lyon-Fedder-Mobarry-simulated reconnection is Petschek like (Ouellette et al., 2010, 2013). Zhang et al. (2016, 2017) have also shown that the rate of reconnection in the magnetosphere is controlled by the solar wind conditions and electrodynamic coupling through the ionosphere rather than the size of the computational cells.

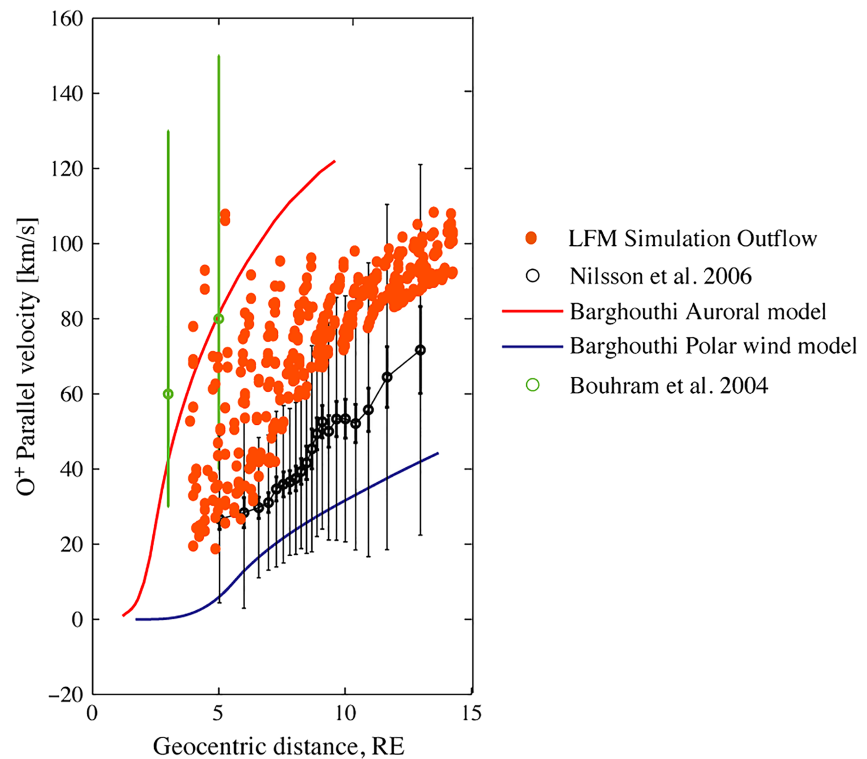


Figure 1. Comparison of outflow velocities versus geocentric distance from the simulation described here, observations, and other simulation models.

The numerical experiment performed in this paper uses similar idealized solar wind and IMF conditions as in Brambles et al. (2011) in order to simulate CME-type driving conditions. After the initially cold, uniform magnetosphere is preconditioned for 4 hr (IMF $B_z = -5$ nT between 00:00 and 02:00 and $B_z = +5$ nT between 02:00 and 04:00 simulation time, ST), IMF B_z is set to be -10 nT for 60 hr (04:00–64:00 ST). The IMF B_x and B_y components are set to 0 and the SW $V_x = -400$ km/s, $V_y = V_z = 0$. The SW number density and sound speed are set to 5 cm $^{-3}$ and 40 km/s, respectively. The dipole tilt angle is 0, and the ionospheric Pedersen conductance is set to be spatially uniform at 5 mho in both hemispheres in order to simplify the analysis. These upstream driving conditions are the same as in Varney et al. (2016a, 2016b) and in case H of Brambles et al. (2011).

The number flux of cusp outflow introduced in the numerical experiment is fixed in time, but its location varies dynamically as determined by a cusp identification algorithm derived from the density enhancement at $2.2 R_E$ (geocentric) (Zhang et al., 2013). For the given SW/IMF conditions, the cusp outflow is mostly located on open field lines near 70° to 75° magnetic latitude and 1130–1230 MLT on the dayside, without significant changes in the cusp area due to the steady-state upstream driving condition. After finding the area of the polar cusp, the O^+ outflow fluid is introduced into the first active computational cell at the low-altitude boundary ($2 R_E$ geocentric) as mass, momentum, and energy fluxes with number density of 150 ions per cubic centimeters, parallel velocity of 18 km/s and temperature of 30 eV.

Figure 1 shows in red dots the simulated outflow parallel velocity along polar-lobe magnetic field lines as a function of geocentric distance overlaid on an adapted version of Figure 1a of Nilsson et al. (2013). The parallel velocity increases to approximately 20–80 km/s at a geocentric distance of $4 R_E$. This range is bracketed at the upper end by the multisatellite observations (green circles) reported by Bouhram et al. (2004) and at the lower end by the CLUSTER observations (black circles) reported by Nilsson et al. (2006). The estimated outflow parallel velocity from auroral and polar wind models (Barghouthi, 2008) are also shown in Figure 1. It is clear that the simulated parallel speed of outflow in the global MHD model is consistent with both observations and other simulation models. The sound speed of the outflowing ions at $4 R_E$ is about 15 km/s, so the flow is supersonic with average Mach number around 2. The specification of cusp outflow in the simulation gives a peak flux of approximately 2.1×10^9 cm 2 /s at an ionospheric reference altitude of

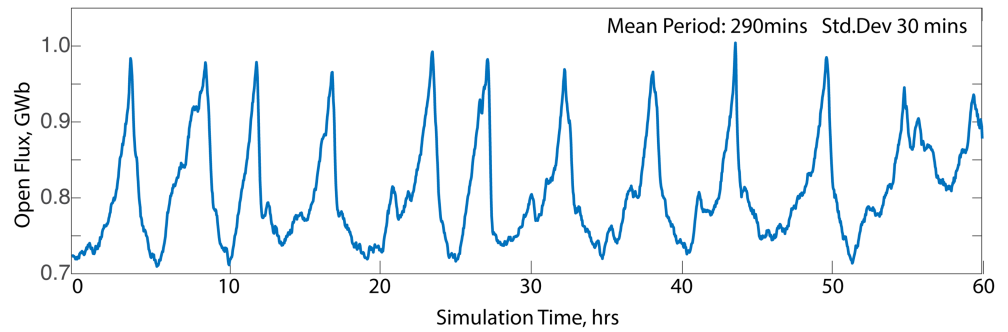


Figure 2. Simulated polar cap open flux versus simulation time in the cusp outflow run.

100 km and a hemispheric outflow rate of approximately $0.72 \times 10^{26} \text{ s}^{-1}$, which is well below the threshold in Brambles et al. (2011) for inducing magnetospheric sawtooth oscillations.

3. Results and Discussions

Figure 2 shows the time variation of the simulated hemispherically integrated, open magnetic flux in the cusp outflow simulation, determined by tracing field lines from the low-altitude boundary of the magnetosphere simulation to magnetic separatrices in the magnetospheric equatorial plane. The enclosed magnetic flux is then calculated using a piecewise constant integral in the polar cap. The simulated open flux in Figure 2 transitions from an SMC state to a sawtooth mode approximately 4 hr after introducing the idealized cusp outflow. The mean period in Figure 2 is between 4–5 hr, which is slightly longer than the mean period (3–4 hr) of observed sawtooth events. The periodicity is characterized by a growth phase wherein the open magnetic flux increases as the lobe magnetic flux compresses the plasma sheet. Onset occurs when the stored open flux in the tail is explosively reconnected. As suggested by Brambles et al. (2011), the longer sawtooth period in the cusp outflow simulation, relative to observations, may be due to the comparatively lower total number of outflowing ions reaching the plasma sheet.

Figure 3a shows a superposed epoch analysis of the simulated open magnetic flux derived from the 10 sawtooth oscillations shown in Figure 2 (cusp outflow + 0.05). For each sawtooth oscillation, onset is identified as the maximum in the polar cap flux and is set as Time = 0 of the epoch. In order to compare with previous results, the simulated open flux shown in Figure 3a has been shifted in the y-axis by plus 0.05 GWb, while the observed open flux reported by Huang et al. (2009) has been shifted in the y-axis by minus 0.15 GWb. This shift of the magnitude of the open flux is only for visualization purpose such that all the three profiles have approximately the same peak flux at Epoche Time = 0. The superposed open flux in the cusp outflow simulation exhibits a change of $\approx 0.2 \text{ GWb}$ during the loading and unloading cycle, which is consistent with the simulations of Brambles et al. (2011) and observations (Huang et al., 2009), especially within $\pm 40 \text{ min}$

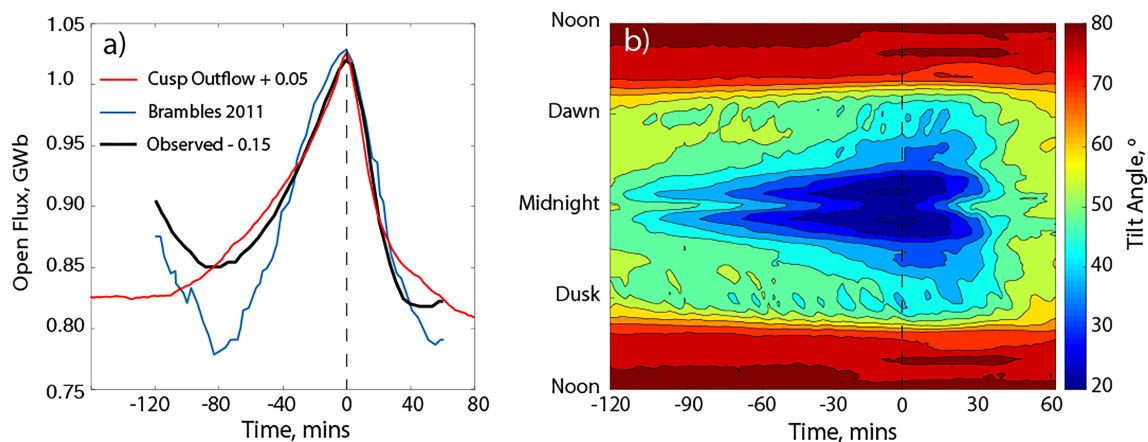


Figure 3. (a) Superposed epoch analysis of open flux during sawtooth oscillations for the cusp outflow simulation, the simulation of Brambles et al. (2011) and observations of Huang et al. (2009). (b) Superposed epoch analysis of magnetic inclination angle near geostationary orbit for the cusp outflow simulation.

of the sawtooth onset time. The similarity indicates that the simulations and observations exhibit the same rate of loading and unloading of magnetic flux.

The wide extent of field line stretching and dipolarization signatures in MLT at geostationary orbit is another distinguishing feature of magnetospheric sawtooth substorms relative to isolated substorms. This feature is also examined for the cusp outflow simulation by comparing a superposed epoch analysis of magnetic inclination angle for the 10 simulated sawtooth oscillations with the corresponding superposed epoch analysis derived from observed sawtooth events (Cai et al., 2006). The magnetic inclination angle is evaluated on the circle $\sqrt{x^2 + y^2} = 6.6 R_E$ in the plane $z = 0.75 R_E$ in the solar-magnetosphere coordinate system for the simulated sawtooth substorms. This analysis is similar to that of Brambles et al. (2011). For each sawtooth, dipolarization onset (Time 0 of the superposed epoch) is visually inferred as the last minimum before the rapid increase in magnetic inclination angle in the 2330 to 0030 MLT sector according to Cai et al. (2006).

The simulated MLT extent of the stretched magnetic field near geostationary orbit (Figure 3b) exhibits a number of similarities compared to the observations (Cai et al., 2006) and simulations of Brambles et al. (2011). The average minimum inclination angle of the simulated sawteeth is approximately 25° as compared to 26° for the observed sawteeth and 27° in Brambles et al. (2011). This minimum inclination angle is much lower than the average minimum of 43° observed at geostationary orbit for isolated substorms. The MLT extent of both the simulated sawtooth oscillations in Brambles et al. (2011) and the observed sawtooth events is comparable; for example, the 44° contour at 0.0 UT in the simulated sawteeth spans approximately 12 hr of MLT, as compared to 12 hr of MLT for the observed sawteeth. However, as a whole, the signatures are not quite as broad compared to either the simulations of Brambles et al. (2011) or the observations (Cai et al., 2006). This discrepancy is likely due to the smaller MLT distribution of outflow in the cusp simulations. The cusp outflow largely lands near the midnight reconnection region in the magnetotail, with less outflow directly filling and stretching the nightside field lines near the geostationary orbit.

Observed sawtooth substorms and the Brambles et al. (2011) results exhibit significant dawn-dusk asymmetry in the MLT distribution of inclination angle, with more pronounced features in the premidnight sector. The sawtooth oscillation induced by cusp outflow in this study is more symmetric across midnight. This difference in dawn-dusk asymmetry is caused by differences in both the ionospheric outflow distributions and the conductance distributions (Lotko et al., 2014) in the two simulation studies. The Brambles et al. (2011) simulations used a causally regulated ionospheric conductance model, which resulted in a dawn-dusk asymmetric outflow distribution and electrodynamic feedback through M-I coupling. The constant conductance used in this study does not allow such asymmetry in the cusp outflow distributions.

The comparisons of open flux and magnetic inclination angle suggest that the mechanism driving the sawtooth oscillations in the cusp outflow simulation is similar to that described by Brambles et al. (2011). The sawtooth substorms in the simulation occur during steady solar wind conditions for which the dayside reconnection potential is relatively constant. The growth in open flux is due to a reduction in the integrated nightside reconnection rate—a consequence of the cusp O^+ ions populating the lobes and plasma sheet. The heavy ions reduce the Alfvén speed in the reconnection inflow region, which reduces the nightside reconnection rate according to the scaling law of Cassak and Shay (2007). As in the Brambles et al. (2011) results, the dayside reconnection rate remains unchanged, but a force imbalance develops due to the accumulation of open magnetic flux in the magnetotail during the growth phase.

The accumulation causes the “widespread” stretching of the plasma sheet field lines registered in Figure 3b. When the open flux becomes sufficiently large, the magnetic field becomes critically stretched, and a plasmoid begins to form on closed field lines. If the last closed field line is subsequently severed, the open lobe flux is reconnected and sawtooth onset occurs. If a plasmoid is formed in the plasma sheet and the open flux is below the critical level, the plasmoid simply flows downtail. None or little open flux is reconnected and sawtooth onset does not occur. Therefore, the period of the simulated sawtooth oscillation is dependent upon the time required for the open flux to reach a critical level, which is controlled by the mass loading of outflowing O^+ and its propensity to decrease the nightside reconnection rate.

This behavior differs from that of isolated substorms, wherein the growth in open flux is caused by a steady southward turning of the IMF and an accompanying increase in the dayside reconnection rate. The

increase in newly opened dayside flux outpaces the latent closing of the nightside flux. This pathway to sub-storm growth and imbalances in dayside and nightside reconnection rates does not require specific spatial distributions of ionospheric outflow, or any outflow.

When ions outflowing from the cusp get trapped in the plasma sheet their inward radial pressure gradient augments the azimuthal current (partial ring current) that distends the nightside magnetic field from dawn to dusk. In the outflow simulation shown in this study, approximately 10% of the outflowing cusp O^+ ions become entrained in the plasma sheet (closed field line region) on average, which is consistent with quantitative estimations from observations (Slapak et al., 2017). Similar to the Brambles et al. (2010) study, when the amount of trapped cusp outflow exceeds a threshold, magnetic field tension can no longer confine the accumulating fluid; an O^+ -rich plasmoid is ejected, with the field subsequently dipolarizing. The results from this simulation clearly show that, even without any nightside outflow contributions, O^+ ions outflowing from the dayside cusp region can also induce magnetospheric sawtooth oscillations. Since the O^+ populations in the simulated plasma sheet all originate from the cusp, the results demonstrate that, in theory, neither nightside outflow, nor causally generated outflow is required to induce magnetospheric sawtooth oscillations. The sole requirement is that O^+ ions have continuous access to the region of nightside reconnection, which is similar to Case B of Brambles et al. (2010).

This cusp outflow requires no feedback mechanism to generate subsequent sawtooth substorms, neither directly as suggested by Varney et al. (2016b) and investigated by Lund et al. (2018) nor indirectly as suggested by Ouellette et al. (2013). However, while nightside outflow released during the expansion phase is not required to produce sawtooth oscillations, its importance in producing the wide MLT signatures has yet to be quantified. Although observations based on several sawtooth events suggested that the ratio of O^+/H^+ remained unchanged between sawtooth oscillations (Liao et al., 2014), future studies are required to clarify the physical role of nightside O^+ ions in the spatial/temporal signatures of magnetospheric sawtooth substorms.

In the numerical experiment discussed here, the magnetospheric response to cusp-only outflow is sensitive to the outflow properties at the inner (low-altitude) simulation boundary. For example, when the outflow density (and flux) in the simulation is doubled, a sawtooth mode is not induced possibly due to the increased momentum causing the plume to simply flow downstream rather than be entrained in nightside reconnection. The physical connections between the cusp outflow rate and the periodicity of the induced sawtooth substorms will be investigated in a follow-up study. Similarly, only a single sawtooth substorm was stimulated in the simulation of Wiltberger et al. (2010) for an outflow flux comparable to the flux in the simulations described here. However, in Wiltberger et al. (2010), the parallel speed of the outflow at the low-altitude boundary was higher (40 km/s) than the 18 km/s velocity in the simulations described here. A higher outflow velocity causes more of the O^+ ions to intersect the equatorial plane downstream of the nightside reconnection line and to flow out the lobes into the solar wind. Such ions have little effect on the nightside reconnection. It is possible that, consistent with Ouellette et al. (2013), nightside outflow may facilitate sawtooth oscillations through pre-conditioning and stretching of the magnetotail, thus allowing more cusp outflow to accumulate in the plasma sheet.

4. Conclusions

The results presented here show that cusp O^+ outflows alone can induce magnetospheric sawtooth substorms in a global geospace simulation. To do so, some portion of the outflowing ions ($\approx 10\%$ in this study) must become entrained in the plasma sheet and modify the nightside reconnection process. Since the simulation does not include a source of nightside outflow, we may conclude from this study that a source of nightside outflow is not required to excite sawtooth substorms. However, nightside outflows may cause sawtooth substorms for some conditions or facilitate their development in concert with dayside outflows.

References

- Barghouthi, I. A. (2008). A Monte Carlo study for ion outflows at high altitude and high latitude: Barghouthi model. *Journal of Geophysical Research*, 113, A08209. <https://doi.org/10.1029/2008JA013274>
- Belian, R. D., Cayton, T. E., & Reeves, G. D. (1995). *Quasi-periodic global substorms generated flux variations observed at geosynchronous orbit* (Vol. 86). Washington D.C.: AGU.
- Borovsky, J. E., Nemzek, R. J., & Belian, R. D. (1993). The occurrence rate of magnetospheric substorm onsets random and periodic substorms. *Journal of Geophysical Research*, 98(A3), 3807–3813. <https://doi.org/10.1029/92ja02556>

Acknowledgments

B. Zhang was supported by the RGC Early Career Scheme (Project 27302018) and RGC the General Research Fund (Project 17300719). Research by W. Lotko and J. Lyon were supported by NASA Grant 80NSSC19K0071. The authors would like to acknowledge high-performance computing support from Cheyenne (doi:10.5065/D6RX99HX) provided by the National Center for Atmospheric Research (NCAR) Computational and Information Systems Laboratory. NCAR is supported by the National Science Foundation. The authors thank Dr. Yuxi Chen for sharing his AGU presentation (posterSM21B-3144 presented at the 2019 Fall Meeting) to provide helpful discussions. The model outputs used to generate the figures for analysis presented in this paper are being preserved online (<https://doi.org/10.5281/zenodo.3595301>).

- Bouhram, M., Klecker, B., Miyake, W., Reme, H., Sauvaud, J. A., Malingre, M., & Blagau, A. (2004). On the altitude dependence of transversely heated O⁺ distributions in the cusp/cleft. *Annales Geophysicae*, 22(5), 1787–1798.
- Brambles, O. J., Lotko, W., Damiano, P. A., Zhang, B., Wiltberger, M., & Lyon, J. (2010). Effects of causally driven cusp O⁺ outflow on the storm time magnetosphere-ionosphere system using a multifluid global simulation. *Journal of Geophysical Research*, 115, A00J04. <https://doi.org/10.1029/2010JA015469>
- Brambles, O. J., Lotko, W., Zhang, B., Ouellette, J., Lyon, J., & Wiltberger, M. (2013). The effects of ionospheric outflow on ICME and SIR driven sawtooth events. *Journal of Geophysical Research: Space Physics*, 118, 6026–6041. <https://doi.org/10.1002/jgra.50522>
- Brambles, O. J., Lotko, W., Zhang, B., Wiltberger, M., Lyon, J., & Strangeway, R. J. (2011). Magnetosphere sawtooth oscillations induced by ionospheric outflow. *Science*, 332(6034), 1183–1186. <https://doi.org/10.1126/science.1202869>
- Cai, X., Henderson, M. G., & Clauer, C. R. (2006). A statistical study of magnetic dipolarization for sawtooth events and isolated substorms at geosynchronous orbit with GOES data. *Annales Geophysicae*, 24(12), 3481–3490.
- Cassak, P. A., & Shay, M. A. (2007). Scaling of asymmetric magnetic reconnection: General theory and collisional simulations. *Physics of Plasmas*, 14, 102114. <https://doi.org/10.1063/1.2795630>
- García, K. S., Merkin, V. G., & Hughes, W. J. (2010). Effects of nightside o⁺ outflow on magnetospheric dynamics: Results of multifluid MHD modeling. *Journal of Geophysical Research*, 115, A00J09. <https://doi.org/10.1029/2010ja015730>
- Henderson, M. G., Reeves, G. D., Skoug, R., Thomsen, M. F., Denton, M. H., Mende, S. B., & Singer, H. J. (2006). Magnetospheric and auroral activity during the 18 April 2002 sawtooth event. *Journal of Geophysical Research*, 111, A01S90. <https://doi.org/10.1029/2005ja011111>
- Huang, C.-S., DeJong, A. D., & Cai, X. (2009). Magnetic flux in the magnetotail and polar cap during sawteeth, isolated substorms, and steady magnetospheric convection events. *Journal of Geophysical Research*, 114, A07202. <https://doi.org/10.1029/2009ja014232>
- Huang, C. S., Reeves, G. D., Borovsky, J. E., Skoug, R. M., Pu, Z. Y., & Le, G. (2003). Periodic magnetospheric substorms and their relationship with solar wind variations. *Journal of Geophysical Research*, 108(A6), 1255. <https://doi.org/10.1029/2002ja009704>
- Kistler, L. M. (2016). The Impact of O⁺ on Magnetotail Dynamics. In C. R. Chappell, R. W. Schunk, P. M. Banks, J. L. Burch, & R. M. Thorne (Eds.), *Magnetosphere-ionosphere coupling in the solar system* (pp. 79–90). Hoboken, New Jersey: John Wiley & Sons, Inc. <https://doi.org/10.1002/9781119066880.ch6>
- Kitamura, K., Kawano, H., Ohtani, S., Yoshikawa, A., & Yumoto, K. (2005). Local time distribution of low and middle latitude ground magnetic disturbances at sawtooth injections of 18–19 April 2002. *Journal of Geophysical Research*, 110, A07208. <https://doi.org/10.1029/2004ja010734>
- Kuznetsova, M. M., Hesse, M., Rastaetter, L., Taktakishvili, A., Toth, G., De Zeeuw, D. L., & Gombosi, T. I. (2007). Multiscale modeling of magnetospheric reconnection. *Journal of Geophysical Research*, 112, A10210. <https://doi.org/10.1029/2007ja012316>
- Liao, J., Cai, X., Kistler, L. M., Clauer, C. R., Mouikis, C. G., Klecker, B., & Dandouras, I. (2014). The relationship between sawtooth events and O⁺ in the plasma sheet. *Journal of Geophysical Research: Space Physics*, 119, 1572–1586. <https://doi.org/10.1002/2013JA019084>
- Lotko, W., Smith, R. H., Zhang, B., Ouellette, J. E., Brambles, O. J., & Lyon, J. G. (2014). Ionospheric control of magnetotail reconnection. *Science*, 345(6193), 184–187. <https://doi.org/10.1126/science.1252907>
- Lund, E. J., Nowrouzi, N., Kistler, L. M., Cai, X., & Frey, H. U. (2018). On the role of ionospheric ions in sawtooth events. *Journal of Geophysical Research: Space Physics*, 123, 665–684. <https://doi.org/10.1002/2017JA024378>
- Lyon, J., Fedder, J., & Mobarry, C. (2004). The Lyon-Fedder-Mobarry (LFM) global MHD magnetospheric simulation code. *Journal of Atmospheric and Solar-Terrestrial Physics*, 66(15-16), 1333–1350. <https://doi.org/10.1016/j.jastp.2004.03.020>
- Nilsson, H., Barghouthi, I. A., Slapak, R., Eriksson, A. I., & André, M. (2013). Hot and cold ion outflow: Observations and implications for numerical models. *Journal of Geophysical Research: Space Physics*, 118, 105–117. <https://doi.org/10.1029/2012JA017975>
- Nilsson, H., Waara, M., Arvelius, S., Marghitu, O., Bouhram, M., Hobara, Y., et al. (2006). Characteristics of high altitude oxygen ion energization and outflow as observed by cluster: A statistical study. *Annales Geophysicae*, 24, 1099–1112. <https://www.ann-geophys.net/24/1099/2006/>
- Ouellette, J. E., Brambles, O. J., Lyon, J. G., Lotko, W., & Rogers, B. N. (2013). (Properties Of outflow driven sawtooth substorms. *Journal of Geophysical Research: Space Physics*, 118, 3223–3232. <https://doi.org/10.1002/jgra.50309>
- Ouellette, J. E., Rogers, B. N., Wiltberger, M., & Lyon, J. G. (2010). Magnetic reconnection at the dayside magnetopause in global lyonfeddermobarry simulations. *Journal of Geophysical Research*, 115, A08222. <https://doi.org/10.1029/2009JA014886>
- Slapak, R., Hamrin, M., Pitkanen, T., Yamauchi, M., Nilsson, H., Karlsson, T., & Schillings, A. (2017). Quantification of the total ion transport in the near-Earth plasma sheet. *Annales Geophysicae*, 35, 869–877. <https://doi.org/10.5194/angeo-35-869-2017>
- Troshichev, O., & Janzhura, A. (2009). Relationship between the PC and AL indices during repetitive bay-like magnetic disturbances in the auroral zone. *Journal of Atmospheric and Solar-Terrestrial Physics*, 71(12), 1340–1352. <https://doi.org/10.1016/j.jastp.2009.05.017>
- Varney, R. H., Wiltberger, M., Zhang, B., Lotko, W., & Lyon, J. (2016a). Influence of ion outflow in coupled geospace simulations: 1. Physics based ion outflow model development and sensitivity study. *Journal of Geophysical Research: Space Physics*, 121, 9671–9687. <https://doi.org/10.1002/2016JA022777>
- Varney, R., Wiltberger, M., Zhang, B., Lotko, W., & Lyon, J. (2016b). Influence of ion outflow in coupled geospace simulations: 2. Sawtooth oscillations driven by physicsbased ion outflow. *Journal of Geophysical Research: Space Physics*, 121, 9688–9700. <https://doi.org/10.1002/2016JA022778>
- Wiltberger, M., Lotko, W., Lyon, J. G., Damiano, P., & Merkin, V. (2010). Influence of cusp O⁺ outflow on magnetotail dynamics in a multifluid MHD model of the magnetosphere. *Journal of Geophysical Research*, 115, A00J05. <https://doi.org/10.1029/2010ja015579>
- Yu, Y., & Ridley, A. J. (2013). Exploring the influence of ionospheric O⁺ outflow on magnetospheric dynamics: Dependence on the source location. *Journal of Geophysical Research: Space Physics*, 118, 1711–1722. <https://doi.org/10.1029/2012JA018411>
- Zhang, B., Brambles, O. J., Cassak, P. A., Ouellette, J. E., Wiltberger, M., Lotko, W., & Lyon, J. G. (2017). Transition from global to local control of dayside reconnection from ionospheric-sourced mass loading. *Journal of Geophysical Research: Space Physics*, 122, 9474–9488. <https://doi.org/10.1002/2016JA023646>
- Zhang, B., Brambles, O., Lotko, W., DunlapShohl, W., Smith, R., Wiltberger, M., & Lyon, J. (2013). Predicting the location of polar cusp in the lyonfeddermobarry global magnetosphere simulation. *Journal of Geophysical Research: Space Physics*, 118, 6327–6337. <https://doi.org/10.1002/jgra.50565>
- Zhang, B., Brambles, O. J., Wiltberger, M., Lotko, W., Ouellette, J. E., & Lyon, J. G. (2016). How does mass loading impact local versus global control on dayside reconnection? *Geophysical Research Letters*, 43, 1837–1844. <https://doi.org/10.1002/2016GL068005>
- Zhang, B., Lotko, W., Brambles, O., Damiano, P., Wiltberger, M., & Lyon, J. (2012). Magnetotail origins of auroral Alfvénic power. *Journal of Geophysical Research*, 117, A09205. <https://doi.org/10.1029/2012JA017680>

- Zhang, B., Lotko, W., Brambles, O., Xi, S., Wiltberger, M., & Lyon, J. (2014). (Solar Wind control of auroral Alfvénic power generated in the magnetotail. *Journal of Geophysical Research: Space Physics*, *119*, 1734–1748. <https://doi.org/10.1002/2013JA019178>
- Zhang, B., Sorathia, K. A., Lyon, J. G., Merkin, V. G., Garretson, J. S., & Wiltberger, M. (2019). GAMERA: A three-dimensional finite-volume MHD solver for non-orthogonal curvilinear geometries. *The Astrophysical Journal Supplement Series*, *244*, 20. <https://doi.org/10.3847/1538-4365/ab3a4c>